LETTER

doi:10.1038/nature10847

Recent contributions of glaciers and ice caps to sea level rise

Thomas Jacob[1]†, John Wahr[1], W. Tad Pfeffer[2,3] & Sean Swenson[4]

Glaciers and ice caps (GICs) are important contributors to present-day global mean sea level rise[1–4]. Most previous global mass balance estimates for GICs rely on extrapolation of sparse mass balance measurements[1,2,4] representing only a small fraction of the GIC area, leaving their overall contribution to sea level rise unclear. Here we show that GICs, excluding the Greenland and Antarctic peripheral GICs, lost mass at a rate of $148 \pm 30\ \mathrm{Gt\ yr^{-1}}$ from January 2003 to December 2010, contributing $0.41 \pm 0.08\ \mathrm{mm\ yr^{-1}}$ to sea level rise. Our results are based on a global, simultaneous inversion of monthly GRACE-derived satellite gravity fields, from which we calculate the mass change over all ice-covered regions greater in area than 100 km^2. The GIC rate for 2003–2010 is about 30 per cent smaller than the previous mass balance estimate that most closely matches our study period[2]. The high mountains of Asia, in particular, show a mass loss of only $4 \pm 20\ \mathrm{Gt\ yr^{-1}}$ for 2003–2010, compared with 47–55 $\mathrm{Gt\ yr^{-1}}$ in previously published estimates[2,5]. For completeness, we also estimate that the Greenland and Antarctic ice sheets, including their peripheral GICs, contributed $1.06 \pm 0.19\ \mathrm{mm\ yr^{-1}}$ to sea level rise over the same time period. The total contribution to sea level rise from all ice-covered regions is thus $1.48 \pm 0.26\ \mathrm{mm\ yr^{-1}}$, which agrees well with independent estimates of sea level rise originating from land ice loss and other terrestrial sources[6].

Interpolation of sparse mass balance measurements on selected glaciers is usually used to estimate global GIC mass balance[1,2,4]. Models are also used[3,7], but these depend on the quality of input climate data and include simplified glacial processes. Excluding Greenland and Antarctic peripheral GICs (PGICs), GICs have variously been reported to have contributed 0.43–0.51 $\mathrm{mm\ yr^{-1}}$ to sea level rise (SLR) during 1961–2004[3,7,8], 0.77 $\mathrm{mm\ yr^{-1}}$ during 2001–2004[8], 1.12 $\mathrm{mm\ yr^{-1}}$ during 2001–2005[1] and 0.95 $\mathrm{mm\ yr^{-1}}$ during 2002–2006[2].

The Gravity Recovery and Climate Experiment (GRACE) satellite mission[9] has provided monthly, global gravity field solutions since 2002, allowing users to calculate mass variations at the Earth's surface[10]. GRACE has been used to monitor the mass balance of selected GIC regions[11–14] that show large ice mass loss, as well as of Antarctica and Greenland[15].

Here we present a GRACE solution that details individual mass balance results for every region of Earth with large ice-covered areas. The main focus of this paper is on GICs, excluding Antarctic and Greenland PGICs. For completeness, however, we also include results for the Antarctic and Greenland ice sheets with their PGICs. GRACE does not have the resolution to separate the Greenland and Antarctic ice sheets from their PGICs. All results are computed for the same 8-yr time period (2003–2010).

To determine losses of individual GIC regions, we cover each region with one or more 'mascons' (small, arbitrarily defined regions of Earth) and fit mass values for each mascon (ref. 16 and Supplementary Information) to the GRACE gravity fields, after correcting for hydrology and for glacial isostatic adjustment (GIA) computed using the ICE-5G deglaciation model. We use 94 monthly GRACE solutions from the University of Texas Center for Space Research, spanning January 2003 to December 2010. The GIA corrections do not include the effects of post-Little Ice Age (LIA) isostatic rebound, which we separately evaluate and remove. All above contributions and their effects on the GRACE solutions are discussed in Supplementary Information.

Figure 1 shows mascons for all ice-covered regions, constructed from the Digital Chart of the World[17] and the Circum-Arctic Map of Permafrost and Ground-Ice Conditions[18]. Each ice-covered region is chosen as a single mascon, or as the union of several non-overlapping mascons. We group 175 mascons into 20 regions. Geographically isolated regions with glacierized areas less than 100 km^2 in area are excluded. Because GRACE detects total mass change, its results for an ice-covered region are independent of the glacierized surface area (Supplementary Information).

Mass balance rates for each region are shown in Table 1 (see Supplementary Information for details on the computation of the rates and uncertainties). We note that Table 1 includes a few positive rates, but none are significantly different from zero. We also performed an inversion with GRACE fields from the GFZ German Research Centre for Geosciences and obtained results that agreed with those from the Center for Space Research (Table 1) to within 5% for each region.

The results in Table 1 are in general agreement with previous GRACE studies for the large mass loss regions of the Canadian Arctic[12] and Patagonia[11], as well as for the Greenland and Antarctic ice sheets with

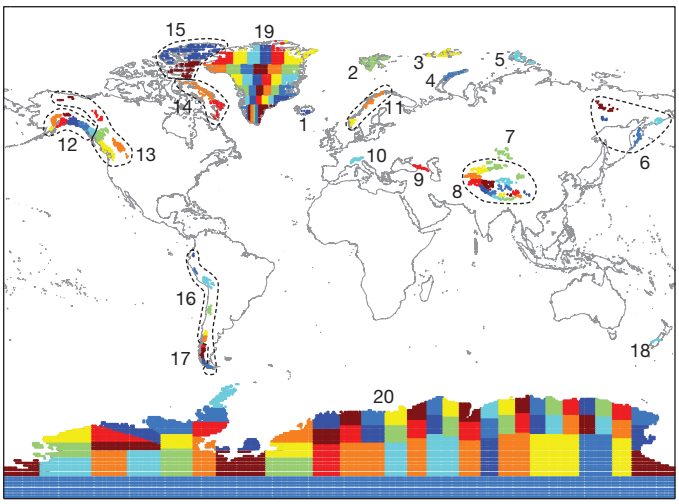

Figure 1 | Mascons for the ice-covered regions considered here. Each coloured region represents a single mascon. Numbers correspond to regions shown in Table 1. Regions containing more than one mascon are outlined with a dashed line.

[1]Department of Physics and Cooperative Institute for Environmental Studies, University of Colorado at Boulder, Boulder, Colorado 80309, USA. [2]Institute of Arctic and Alpine Research, University of Colorado at Boulder, Boulder, Colorado 80309, USA. [3]Department of Civil, Environmental, and Architectural Engineering, University of Colorado at Boulder, Boulder, Colorado 80309, USA. [4]National Center for Atmospheric Research, Boulder, Colorado 80305, USA. †Present address: Bureau de Recherches Géologiques et Minières, Orléans 45060, France.

Table 1 | Inverted 2003–2010 mass balance rates

Region	Rate (Gt yr^{-1})
1. Iceland	−11 ± 2
2. Svalbard	−3 ± 2
3. Franz Josef Land	0 ± 2
4. Novaya Zemlya	−4 ± 2
5. Severnaya Zemlya	−1 ± 2
6. Siberia and Kamchatka	2 ± 10
7. Altai	3 ± 6
8. High Mountain Asia	−4 ± 20
8a. Tianshan	−5 ± 6
8b. Pamirs and Kunlun Shan	−1 ± 5
8c. Himalaya and Karakoram	−5 ± 6
8d. Tibet and Qilian Shan	7 ± 7
9. Caucasus	1 ± 3
10. Alps	−2 ± 3
11. Scandinavia	3 ± 5
12. Alaska	−46 ± 7
13. Northwest America excl. Alaska	5 ± 8
14. Baffin Island	−33 ± 5
15. Ellesmere, Axel Heiberg and Devon Islands	−34 ± 6
16. South America excl. Patagonia	−6 ± 12
17. Patagonia	−23 ± 9
18. New Zealand	2 ± 3
19. Greenland ice sheet + PGICs	−222 ± 9
20. Antarctica ice sheet + PGICs	−165 ± 72
Total	−536 ± 93
GICs excl. Greenland and Antarctica PGICs	−148 ± 30
Antarctica + Greenland ice sheet and PGICs	−384 ± 71
Total contribution to SLR	1.48 ± 0.26 mm yr^{-1}
SLR due to GICs excl. Greenland and Antarctica PGICs	0.41 ± 0.08 mm yr^{-1}
SLR due to Antarctica + Greenland ice sheet and PGICs	1.06 ± 0.19 mm yr^{-1}

Uncertainties are given at the 95% (2σ) confidence level.

their PGICs[19]. Our results for Alaska also show considerable mass loss, although our mass loss rate is smaller than some previously published GRACE-derived rates that used shorter and earlier GRACE data spans (Supplementary Information). The global GIC mass balance, excluding Greenland and Antarctic PGICs, is -148 ± 30 Gt yr^{-1}, contributing 0.41 ± 0.08 mm yr^{-1} to SLR.

Mass balance time series for all GIC regions are shown in Fig. 2. The seasonal and interannual variabilities evident in these time series have contributions from ice and snow variability on the glaciers, as well as from imperfectly modelled hydrological signals in adjacent regions and from random GRACE observational errors. Interannual variability can affect rates determined over short time intervals. Figure 2 and Supplementary Table 2 show that there was considerable interannual variability during 2003–2010 for some of the regions, especially High Mountain Asia (HMA). The HMA results in Supplementary Table 2 show that this variability induces large swings in the trend solutions when it is fitted to subsets of the entire time period. These results suggest that care should be taken in extending the 2003–2010 results presented in this paper to longer time periods.

For comparison with studies in which PGICs are included with GICs, we upscale our GIC-alone rate to obtain a GIC rate that includes PGIC, based on ref. 3 (Supplementary Information). The result is that GICs including PGICs lost mass at a rate of 229 ± 82 Gt yr^{-1} (0.63 ± 0.23 mm yr^{-1} SLR), and that the combined ice sheets without their PGICs lost mass at 303 ± 100 Gt yr^{-1} (0.84 ± 0.28 mm yr^{-1} SLR). Although no other study encompasses the same time span, published non-GRACE estimates for GICs plus PGICs are larger: 0.98 ± 0.19 mm yr^{-1} over 2001–2004[8], 1.41 ± 0.20 mm yr^{-1} over 2001–2005[1] and 0.765 mm yr^{-1} (no uncertainty given) over 2006–2010[20]. These differences could be due to the small number of mass balance measurements those estimates must rely on, combined with uncertain regional glacier extents. In addition, there are indications from more recent non-GRACE measurements that the GIC mass loss rate decreased markedly beginning in 2005[20].

Our results for HMA disagree significantly with previous studies. A recent GRACE-based study[5] over 2002–2009 yields significantly

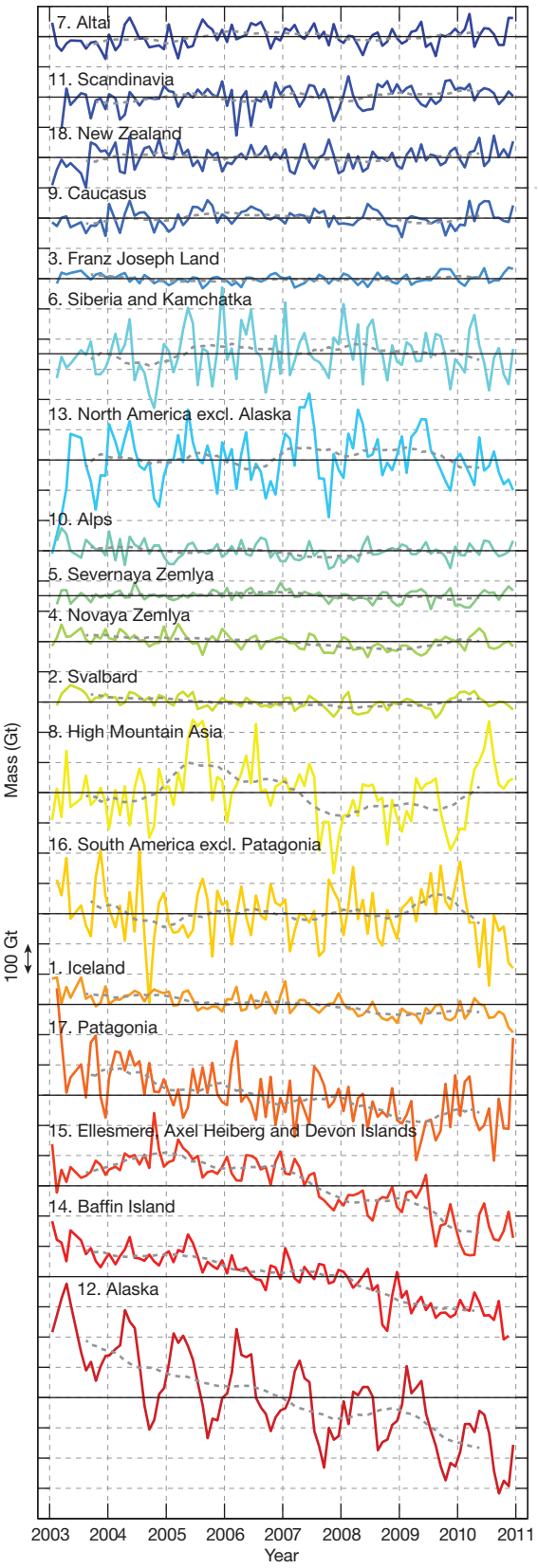

Figure 2 | Mass change during 2003–2010 for all GIC regions shown in Fig. 1 and Table 1. The black horizontal lines run through the averages of the time series. The grey lines represent 13-month-window, low-pass-filtered versions of the data. Time series are shifted for legibility. Modelled contributions from GIA, LIA and hydrology have been removed.

larger mass loss for HMA than does ours; we explain why the result of ref. 5 may be flawed in Supplementary Information. Conventional mass balance methods have been used to estimate a 2002–2006 rate of $-55\,\mathrm{Gt\,yr^{-1}}$ for this entire region[2], with $-29\,\mathrm{Gt\,yr^{-1}}$ over the eastern Himalayas alone, by contrast with our HMA estimate, of $-4 \pm 20\,\mathrm{Gt\,yr^{-1}}$ (Table 1). We show results for the four subregions of HMA (Fig. 3) in Table 1.

This difference prompts us to examine this region in more detail. GRACE mass trends show considerable mass loss across the plains of northern India, Pakistan and Bangladesh, centred south of the glaciers and at low elevations (Fig. 3a, b). Some of the edges of this mass loss region seem to extend over adjacent mountainous areas to the north, but much of that, particularly above north-central India, is leakage of the plains signal caused by the 350-km Gaussian smoothing function used to generate the figure. The plains signal has previously been identified as groundwater loss[16,21]. To minimize leakage in the HMA GIC estimates, additional mascons are chosen to cover the plains (Fig. 3a), the sum of which gives an average 2003–2010 water loss rate of $35\,\mathrm{Gt\,yr^{-1}}$. Our plains results are consistent with the results of refs 16 and 21, which span shorter time periods.

The lack of notable mass loss over glacierized regions is consistent with our HMA mascon solutions that indicate relatively modest losses (Table 1). We simulate what the ice loss rates predicted by ref. 2 would look like in the GRACE results. We use those rates to construct synthetic gravity fields and process them using the same methods applied to the GRACE data, to generate the trend map shown in Fig. 3c. It is apparent that an ice loss of this order would appear in the GRACE map as a large mass loss signal centred over the eastern Himalayas, far larger in amplitude and extent than the GRACE results in that region (compare Fig. 3b with Fig. 3c).

It is reasonable to wonder whether a tectonic process could be causing a positive signal in the glacierized region that offsets a large negative glacier signal in HMA. To see what this positive rate would have to look like, we remove the simulated gravity field (based on ref. 2) from the GRACE data and show the resulting difference map in Fig. 3d. If the ice loss estimate were correct, the tectonic process would be causing an anomalous mass increase over the Himalayas of $\sim 3\,\mathrm{cm\,yr^{-1}}$ equivalent water thickness, equivalent to $\sim 1\,\mathrm{cm\,yr^{-1}}$ of uncompensated crustal uplift. Although we cannot categorically rule out such a possibility, it seems unlikely. Global Positioning System and levelling observations in this region indicate long-term uplift rates as large as 0.5–0.7 $\mathrm{cm\,yr^{-1}}$ in some places[22,23]. But it is highly probable that any broad-scale tectonic uplift would be isostatically compensated by an increasing mass deficiency at depth, with little net effect on gravity[24] and, consequently, no significant contribution to the GRACE results. The effects of compensation are evident in the static gravity field. Supplementary Fig. 4

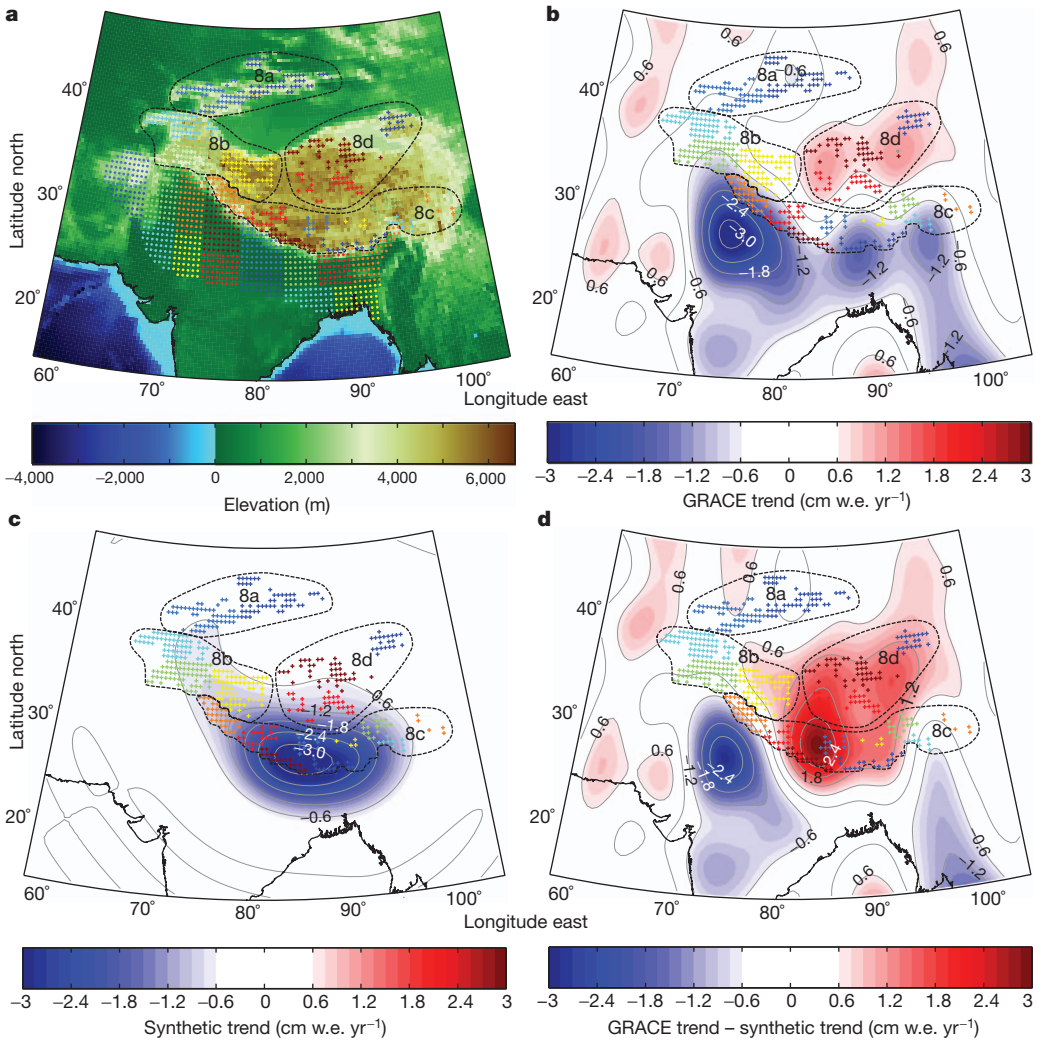

Figure 3 | HMA mass balance determination. **a**, Topographic map overlaid with the HMA mascons (crosses) and India plain mascons (dots); the dashed lines delimit the four HMA subregions (labelled as in Table 1). **b**, GRACE mass rate corrected for hydrology and GIA and smoothed with a 350-km Gaussian smoothing function, overlaid with the HMA mascons. w.e., water equivalent. **c**, Synthetic GRACE rates that would be caused by a total mass loss of $55\,\mathrm{Gt\,yr^{-1}}$ over HMA mascons, with $29\,\mathrm{Gt\,yr^{-1}}$ over the eastern Himalayas, after ref. 2. **d**, The difference between **b** and **c**.

shows the free-air gravity field, computed using a 350-km Gaussian smoothing function (used to generate Fig. 3) applied to the EGM96 mean global gravity field[25]. The topography leaves no apparent signature on the static gravity field at these scales, indicating near-perfect compensation.

For a solid-Earth process to affect GRACE significantly, it must be largely isostatically uncompensated, which for these broad spatial scales would require characteristic timescales of the same order or less than the mantle's viscoelastic relaxation times (several hundred to a few thousand years). One possible such process might be the ongoing viscoelastic response of the Earth to past glacial unloading. We have investigated this effect, as well as possible contributions from erosion, and find that neither is likely to be important (Supplementary Information).

Another possible explanation for the lack of a large GRACE HMA signal is that most of the glacier melt water might be sinking into the ground before it has a chance to leave the glaciated region, thus causing GRACE to show little net mass change. Some groundwater recharge undoubtedly does occur, but it seems unlikely that such cancellation would be this complete. Much of HMA, for example, is permafrost, so local storage capacity is small (see the Circum-Arctic Map of Permafrost and Ground-Ice Conditions; http://nsidc.org/fgdc/maps/ipa_browse.html). Therefore, although there would be surface melt, the frozen ground would inhibit local recharge and there would be little ability to store the melt water locally. How far the water might have to travel before finding recharge pathways, we do not know. It is true that some rivers originating in portions of HMA do not reach the sea. Most notable are the Amu Darya and Syr Darya, which historically feed the Aral Sea but have been diverted for irrigation. Any fraction of that diverted water that ends up recharging aquifers will not directly contribute to SLR. However, the irrigation areas lie well outside our HMA mascons, and so even if there is notable recharge it is unlikely to affect the HMA mascon solutions significantly.

Our emphasis here is on GICs; the Greenland and Antarctic ice sheets have previously been well studied with GRACE[15]. But for comparison with non-GRACE global estimates, we combine our GIC results with our estimates for Greenland plus Antarctica to obtain a total SLR contribution from all ice-covered regions of $1.48 \pm 0.26\,\mathrm{mm\,yr^{-1}}$ during 2003–2010. Within the uncertainties, this value compares favourably with the estimate of $1.8 \pm 0.5\,\mathrm{mm\,yr^{-1}}$ for 2006 from ref 4. However, there are regional differences between these and prior results, which need further study and reconciliation.

SLR from the addition of new water can be determined from GRACE alone as well as by subtracting Argo steric heights from altimetric SLR measurements[6]. The most recent new-water SLR estimate, comparing the two methods, is $1.3 \pm 0.6\,\mathrm{mm\,yr^{-1}}$ for 2005–2010[6], which agrees with our total ice-covered SLR value to within the uncertainties. The difference, $0.2 \pm 0.6\,\mathrm{mm\,yr^{-1}}$, could represent an increase in land water storage outside ice-covered regions, but we note that it is not significantly different from zero.

METHODS SUMMARY

GRACE solutions consist of spherical harmonic (Stokes) coefficients and are used to determine month-to-month variations in Earth's mass distribution[9,10]. We use monthly values of C_{20} (the zonal, degree-2 spherical harmonic coefficient of the geopotential) from satellite laser ranging[26], and include degree-one terms[27].

To determine mass variability for each mascon, we find the set of Stokes coefficients produced by a unit mass distributed uniformly across that mascon. We fit these sets of Stokes coefficients, simultaneously, to the GRACE Stokes coefficients, to obtain monthly mass values for each mascon. This method is similar to previously published mascon methods[28], though here we fit to Stokes coefficients rather than to raw satellite measurements and we do not impose smoothness constraints. To determine the optimal shape and number of mascons in a region, we construct a sensitivity kernel for several possible configurations, and choose the configuration that optimizes that kernel and minimizes the GRACE trend residuals (Supplementary Fig. 1c).

The average of two land surface models is used to correct for hydrology, and the model differences are used to estimate uncertainties (Supplementary Information).

LIA loading corrections have been previously derived for Alaska[13] and Patagonia[29], and equal 7 and 9 $\mathrm{Gt\,yr^{-1}}$, respectively. These numbers are subtracted from our Alaska and Patagonia inversions. For other GIC regions, where LIA characteristics are not well known, we estimate an upper bound for the correction by constructing a GIA model that tends to maximize the positive LIA gravity trend. Of all the additional GIC regions, only HMA has a predicted LIA correction that reaches 1 $\mathrm{Gt\,yr^{-1}}$. There, the model suggests we remove 5 $\mathrm{Gt\,yr^{-1}}$ from our inverted result. But because the LIA correction in this region is likely to be an overestimate (Supplementary Information), our preferred result splits the difference (Supplementary Table 1), and we use that difference to augment the total HMA uncertainty.

Received 28 July 2011; accepted 9 January 2012.
Published online 8 February 2012.

1. Cogley, J. G. Geodetic and direct mass-balance measurements: comparison and joint analysis. *Ann. Glaciol.* **50,** 96–100 (2009).
2. Dyurgerov, M. B. Reanalysis of glacier changes: from the IGY to the IPY, 1960–2008. *Data Glaciol. Stud.* **108,** 1–116 (2010).
3. Hock, R., de Woul, M., Radic, V. & Dyurgerov, M. Mountain glaciers and ice caps around Antarctica make a large sea-level rise contribution. *Geophys. Res. Lett.* **36,** L07501 (2009).
4. Meier, M. F. *et al.* Glaciers dominate eustatic sea-level rise in the 21st century. *Science* **317,** 1064–1067 (2007).
5. Matsuo, K. & Heki, K. Time-variable ice loss in Asian high mountains from satellite gravimetry. *Earth Planet. Sci. Lett.* **290,** 30–36 (2010).
6. Willis, J. K., Chambers, D. P., Kuo, C. Y. & Shum, C. K. Global sea level rise, recent progress and challenges for the decade to come. *Oceanography (Wash. DC)* **23,** 26–35 (2010).
7. Hirabayashi, Y., Doll, P. & Kanae, S. Global-scale modeling of glacier mass balances for water resources assessments: glacier mass changes between 1948 and 2006. *J. Hydrol. (Amst.)* **390,** 245–256 (2010).
8. Kaser, G., Cogley, J. G., Dyurgerov, M. B., Meier, M. F. & Ohmura, A. Mass balance of glaciers and ice caps: consensus estimates for 1961–2004. *Geophys. Res. Lett.* **33,** L19501 (2006).
9. Tapley, B. D., Bettadpur, S., Watkins, M. & Reigber, C. The gravity recovery and climate experiment: mission overview and early results. *Geophys. Res. Lett.* **31,** L09607 (2004).
10. Wahr, J., Swenson, S., Zlotnicki, V. & Velicogna, I. Time-variable gravity from GRACE: first results. *Geophys. Res. Lett.* **31,** L11501 (2004).
11. Chen, J. L., Wilson, C. R., Tapley, B. D., Blankenship, D. D. & Ivins, E. R. Patagonia icefield melting observed by gravity recovery and climate experiment (GRACE). *Geophys. Res. Lett.* **34,** L22501 (2007).
12. Gardner, A. S. *et al.* Sharply increased mass loss from glaciers and ice caps in the Canadian Arctic Archipelago. *Nature* **473,** 357–360 (2011).
13. Luthcke, S. B., Arendt, A. A., Rowlands, D. D., McCarthy, J. J. & Larsen, C. F. Recent glacier mass changes in the Gulf of Alaska region from GRACE mascon solutions. *J. Glaciol.* **54,** 767–777 (2008).
14. Riva, R. E. M., Bamber, J. L., Lavallee, D. A. & Wouters, B. Sea-level fingerprint of continental water and ice mass change from GRACE. *Geophys. Res. Lett.* **37,** L19605 (2010).
15. Rignot, E., Velicogna, I., van den Broeke, M. R., Monaghan, A. & Lenaerts, J. Acceleration of the contribution of the Greenland and Antarctic ice sheets to sea level rise. *Geophys. Res. Lett.* **38,** L05503 (2011).
16. Tiwari, V. M., Wahr, J. & Swenson, S. Dwindling groundwater resources in northern India, from satellite gravity observations. *Geophys. Res. Lett.* **36,** L18401 (2009).
17. Raup, B. H., Kieffer, H. H., Hare, J. M. & Kargel, J. S. Generation of data acquisition requests for the ASTER satellite instrument for monitoring a globally distributed target: glaciers. *IEEE Trans. Geosci. Remote Sens.* **38,** 1105–1112 (2000).
18. Brown, J., Ferrians, O. J., Heginbottom, J. A. & Melnikov, E. S. *Circum-Arctic Map of Permafrost and Ground-Ice Conditions.* National Snow and Ice Data Center/World Data Center for Glaciology (1998, revised, February 2001).
19. Velicogna, I. Increasing rates of ice mass loss from the Greenland and Antarctic ice sheets revealed by GRACE. *Geophys. Res. Lett.* **36,** L19503 (2009).
20. Cogley, J. G. in *Future Climates of the World* (eds Henderson-Sellers, A. & McGuffie, K.) 189–214 (Elsevier, 2012).
21. Rodell, M., Velicogna, I. & Famiglietti, J. S. Satellite-based estimates of groundwater depletion in India. *Nature* **460,** 999–1002 (2009).
22. Bettinelli, P. *et al.* Plate motion of India and interseismic strain in the Nepal Himalaya from GPS and DORIS measurements. *J. Geod.* **80,** 567–589 (2006).
23. Jackson, M. & Bilham, R. Constraints on Himalayan deformation inferred from vertical velocity-fields in Nepal and Tibet. *J. Geophys. Res. Solid Earth* **99,** 13897–13912 (1994).
24. Zhong, S. J. & Zuber, M. T. Crustal compensation during mountain-building. *Geophys. Res. Lett.* **27,** 3009–3012 (2000).
25. Lemoine, F. *et al. The Development of the Joint NASA GSFC and NIMA Geopotential Model EGM96.* NASA Goddard Space Flight Center (1998).
26. Cheng, M. K. & Tapley, B. D. Variations in the Earth's oblateness during the past 28 years. *J. Geophys. Res.* **109,** B09402 (2004).
27. Swenson, S., Chambers, D. & Wahr, J. Estimating geocenter variations from a combination of GRACE and ocean model output. *J. Geophys. Res. Solid Earth* **113,** B08410 (2008).

28. Rowlands, D. D. *et al.* Resolving mass flux at high spatial and temporal resolution using GRACE intersatellite measurements. *Geophys. Res. Lett.* **32,** L04310 (2005).
29. Ivins, E. R. & James, T. S. Bedrock response to Llanquihue Holocene and present-day glaciation in southernmost South America. *Geophys. Res. Lett.* **31,** L24613 (2004).

Supplementary Information is linked to the online version of the paper at www.nature.com/nature.

Acknowledgements We thank Geruo A for providing the glacial isostatic adjustment model, and G. Cogley, G. Kaser, I. Velicogna, T. Perron and M. Tamisiea for comments. This work was partially supported by NASA grants NNX08AF02G and NNXI0AR66G, and by NASA's 'Making Earth Science Data Records for Use in Research Environments (MEaSUREs) Program'.

Author Contributions T.J. and J.W. developed the study and wrote the paper. W.T.P. and S.S. discussed, commented on and improved the manuscript. S.S. provided the CLM4 hydrology model output.

Author Information Reprints and permissions information is available at www.nature.com/reprints. The authors declare no competing financial interests. Readers are welcome to comment on the online version of this article at www.nature.com/nature. Correspondence and requests for materials should be addressed to J.W. (john.wahr@gmail.com).